Toughness and Ductility of Fibre Reinforced Cementitious Composites in Flexure

Jalil Morshedian and Mohammad Razavy Nouri
Polymer Research Center of Iran, Tehran, I.R. Iran

Received: 21 April 1993, accepted 24 July 1993

ABSTRACT

An experimental and theoretical study of the post-cracking behaviour and ductility of fibre reinforced cementitious beams in flexure is reported. Flexural loading tests have been conducted on notched beams containing varying amounts of E-glass,Dolanit 10 and 11 fibres (Hoechst Polyacrylonitrile Fiber Products). The test data were analysed to evaluate the effect of fibre type and fibre volume on the toughness and ductility of fibre-reinforced cementitious composites. A theoretical model has been proposed and found to fit the test data appropriately.

Key Words

energy absorption, post-cracking, stress intensity factor, cementitious composites, ductility

INTRODUCTION

Cement and cementitious-based fibre composites are basically discontinuous, anisotropic, heterogeneous, multi-phase systems. Such materials contain interfacial bond micro-cracks and other inherent flaws arising from volume changes and those effects taking place during fabrication process. It is these bond microcracks and interfacial discontinuities which create through their geometry the nuclei for potential crack propagation and fracture [1, 2]. When such materials are subjected to external loading , the existing micro-cracks progressively increase and grow, during which energy is dissipated by different mechanisms. Such materials display non-linear stress-strain behaviour, and a semi-ductile mode of failure in contrast to the brittle or Griffith material in which the onset of crack growth is synonymous with fracture. The strength, stiffness and mode of failure of such materials are also affected by the size of specimen considered [3,4].

The conventional Griffith concept cannot be applied to cement and fibre- cement (concrete) composite fracture should not be able to quantify the various energy dissipating mechanisms involved. The cement paste matrix, the nearest to a homogeneous elastic material in the concrete system, is itself not a truly brittle material. Indeed in notched samples considerable micro-cracking

occurs at a crack tip and in the presence of aggregate in concrete and /or fibre inclusions in concrete there is considerable stress transfer across the aggregate-matrix interfacial cracking which cannot be ignored in cement-based fibre composites, whether the composite failure occurs by fibre pull-out or fibre fracture [5,6].

However, several linear-elastic fracture mechanics have been applied to cement paste, mortars and concrete as well as to fibre cement composites. The results obtained by different investigators show a wide range of experimental values for the critical rate of release of elastic strain energy with respect to the crack length (Gc), which probably confirm that some forms of energy dissipation other than surface energy are involved which are not accounted for in the failure of cement-based composites. It is, however, recognised that the "pseudo- plastic" zone immediately in front of the crack tip can be considerably large in relation to the flaw size and size of the test member, and indeed may control the strength of the composites [7]. It is then obvious that the linear fracture mechanics approach is not valid for such cases.

In this work a theoretical model is introduced to represent the toughness, i.e. capacity of energy absorption and ductility of fibre reinforced cementitious composites. This model is employed for notched fibre reinforced cementitious beams subjected to flexural loading and will be shown to suitably satisfy the test data.

EXPERIMENTAL

A portland cement with a specific surface area of about 2500 cm^2/g was used in making the specimens. The chemical compositions and physical properties of the portland cement are given in Table 1.

From the chemical compositions of cement and Bouge equations [8], the amounts of C_2S, C_3S, C_4AF and C_3A can be calculated. These values are given in Table 2.

Two types of PAN fibres of different diameters (Dolanit 10 and 11) were used. The E-glass, Dolanit 11 and Dolanit 10 were in the form of chopped rovings, 6mm long and 18μm, 104μm, 18μm in diameter, respectively. The E-glass and Dolanit 10 were used in volume fraction of 1%, 2% and 3% and Dolanit 11 was used in

Table 1. Chemical compositions and physical properties of portland cement.

Chemical Compositions (%)							
Ign.loss	SiO_2	Al_2O_3	Fe_2O_3	CaO	MgO	SO_3	Free lime
2.05	20.84	3.85	5.4	62.44	1.4	4.16	1.49

Physical Properties	
Specific gravity (20 °C)	Specific surface area (cm^2/g)
3.12	2500

Table 2. Percentage of main compounds in portland cement.

$3CaO.SiO_2$	$2CaO.SiO_2$	$3CaO.Al_2O_3$	$4CaO.Al_2O_3.Fe_2O_3$
(C_3S)	(C_2S)	(C_3A)	(C_4AF)
50.37	21.85	1.07	16.43

volume fractions of 1%, 3%, 5% and 6%. Mixing was carried out conventionally in an electrically driven mechanical mixer of epicyclic type which imparted both a rotary and a revolving motion to the mixer paddle. The cement matrix was mixed with fibres and water with 0.3 water to cement ratio. When cement was added to the water and mixed, the fibres were sprinkled randomly into the cement matrix and after 3 minutes, mixing was completed. All specimens were made in steel moulds. Control specimens (without fibres) were also made for carrying out comparison tests. All the specimens were compacted by table vibration and had 160 x 90 x 40 mm final dimensions. The notches were cut with a dimond saw at the centre of one of the faces of the specimen. All the test specimens were provided with a notch 2mm wide and 10mm deep over the full width of the beam. The test specimens were demoulded after 24 hours at room temperature, cured in a water bath at a temperature of 20 $\pm$ 2 °C and then tested after six days immersion.

At least three specimens were tested for each fibre volume. All the tests reported here were carried out at the same constant deflection rate (1mm/min) in three point bending mode with the notches on the tension side by use of an Instron Universal Testing Machine, Model 6025, 10KN load cell.

RESULTS

Among the very large number of data obtained from the tests, only typical results are presented here. Typical load-deflection curves of notched fibre reinforced cementitious beams containing different percentages of E-glass and Dolanit 10 and 11 are shown in Figures 1 to 3.

All the experimental load-deflection curves showed that the post-cracking behaviour and ductility (i.e., the ability of a material to be plastically deformed by elongation without fracture) of the notched beams were influenced by the type of fibre and fibre content.

DISCUSSION

The results indicate that all the experimental data

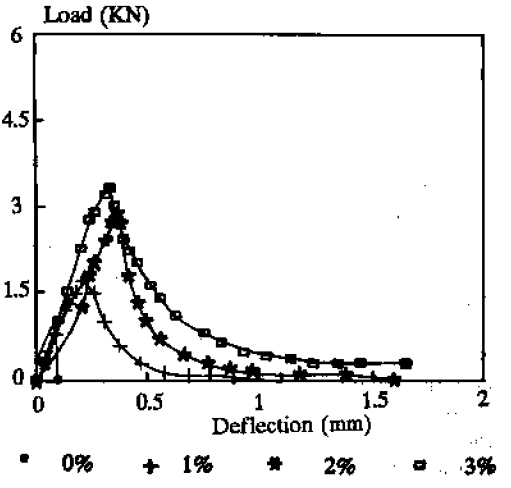

Fig.1. Load-deflection characteristics of notched Dolanit 10 fibre reinforced cementitious beam in flexure.

can be closely approximated to one of three ductile behaviours shown in Figure 4. This figure is a schematic representation of the post-cracking ductility of the cementitious composites as affected by fibre reinforcement [6].

Figure 4 identifies three distinct stages in the load-deflection pattern of a notched beam in flexure. The first stage, during which, the behaviour is linear, characterises the energy content required to just initiate cracking, i.e., it represents the stage when the existing crack length starts to grow. The second stage represents the duration in which the initial crack progresses up to the maximum load and characterises the energy requirement for sub-critical crack growth. This stage is practically negligible in the case of plain concrete in which the onset of fracture is synonymous with initiation of cracking as far as the energy absorption capacity is concerned [6].

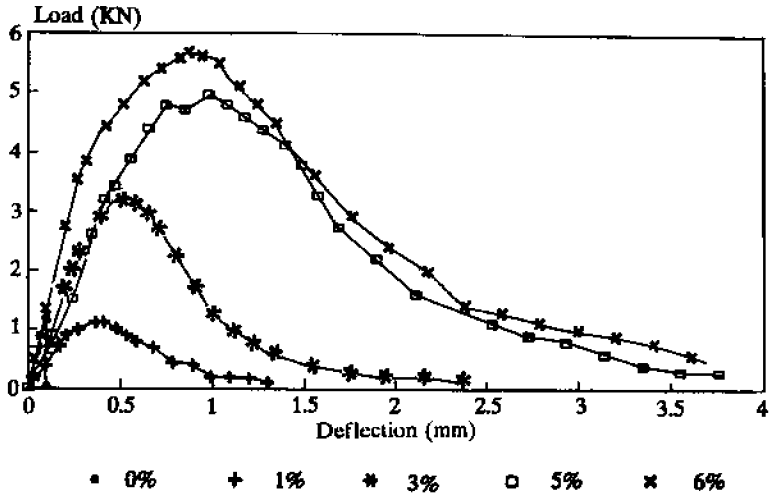

Fig.2. Load-deflection characteristics of notched Dolanit 11 fibre reinforced cementitious beam in flexure.

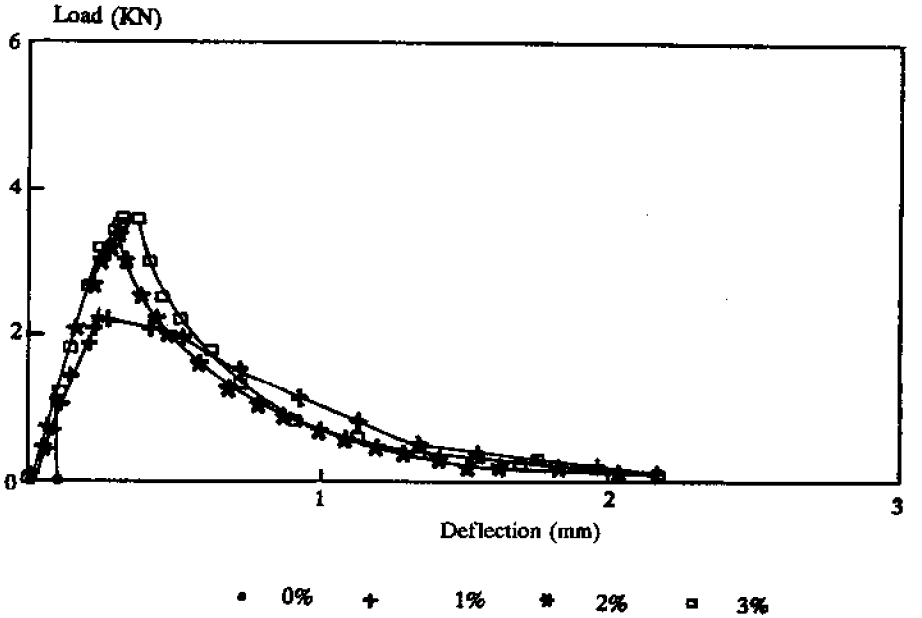

Fig.3. Load-deflection characteristics of notched E-glass fibre reinforced cementitious beam in flexure.

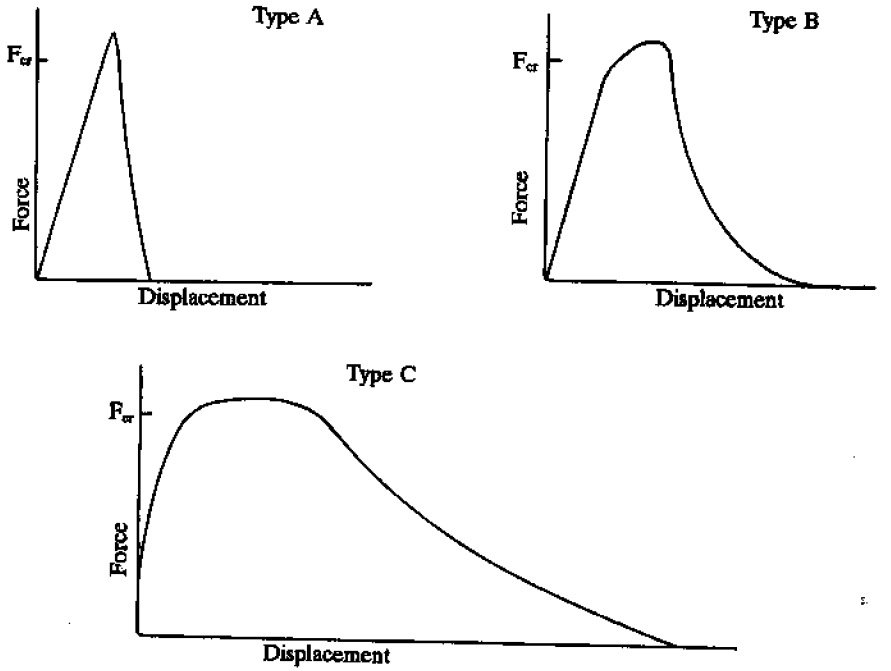

Fig.4. Schematic representation of typical load- displacement curves of notched fibre reinforced cementitious beams in flexure [6].

During this stage, the load increases to a maximum value, though at a lower rate compared to the first stage. The third stage, i.e., beyond the maximum load up to failure, denotes the energy absorption during unstable crack growth and propagation. In this post-yield deformation stage, changes in surface energy due to progressive debonding, the energy dissipation due to friction damping at the interfaces and the inelastic definition at the interface discontinuities, all contribute to progressive micro-cracking and failure. It can be seen that load-deflection behaviour of cement matches with type A and that of Dolanit 10 and E-glass with type B, and finally, the behaviour and Dolanit 11 is similar to fracture behaviour of type C in Figure 4. To quantify the total energy absorption of a specimen before failure, it is necessary to quantify the energy content in each of the three stages. An expression is derived as follows for the energy E_T, i.e., the energy requirement in stages one and two together. However, the energy requirement in the third stage cannot be so easily quantified in simple terms so as to be of any engineering use since it is related to an instability condition. It is, however, to be recognised that even in this stage it is possible to obtain states of quasi-stability.

Because of the unstable conditions in the third stage, the energy absorption is best represented as a ratio of the total energy to the energy E_T, up to the end of stable crack growth. Denoting by F the load and F_{cr} the load at the initiation of crack length increase, the ratio F/F_{cr} gives the load increases beyond stage one up to the

maximum load. If C denotes the specimen compliance which is constant during the first stage, the energy absorbed, E_1 is given by:

$$E_1 = 1/2.C.F_{cr}^2 \quad (1)$$

If ζ denotes the displacement, beyond crack initiation stage (called the post-cracking displacement), then the energy absorption E_2 during the sub-critical crack-growth can be easily shown to be:

$$E_2 = \int_0^{\zeta_m} F.d\zeta \quad (2)$$

or

$$E_2 = F_{cr} \int_0^{\zeta_m} (F/F_{cr}).d\zeta \quad (3)$$

where ζ_m is the displacement corresponding to maximum load less than that corresponding to F_{cr}. E_T is then given by:

$$E_T = E_1 + E_2 = 1/2.C.F_{cr}^2 + F_{cr} \int_0^{\zeta_m} (F/F_{cr}).d\zeta \quad (4)$$

To evaluate E_T from equation (4), it is necessary to know the relation between F/F_{cr} and ζ as relevant to the material under consideration. In Figures 5 to 7, the test data are plotted for cement with E-glass, Dolanit 10 and 11 and it can be noted that the variation of ζ with F/F_{cr} can be closely approximated by the equations:

$$F/F_{cr} = 0.99 + 3.06\,\zeta \quad (5)$$
$$F/F_{cr} = 1.217 + 1.038\,\zeta \quad (6)$$
$$F/F_{cr} = 1.023 + 1.109\,\zeta \quad (7)$$

Corresponding to Dolanit 10 and 11 and E-glass, respectively.

Typical flexural data for beam specimens with notches and those from theoretical manipulation are presented in Table 3. The theoretical and experimental energy absorption values up to the end of subcritical crack growth stage are also shown in Table 3. The agreement

Table 3. Typical results of notched fibre reinforced cementitious beams in flexure.

Type of fibre	Fibre volume (%)	F_{cr} (N)	Energy capacity up to end of sub-critical crack growth stage (E_T) Theoretical (N.mm)	Energy capacity up to end of sub-critical crack growth stage (E_T) Experimental (N.mm)	Total energy for failure of beams Experimental (N.mm)	E_T (Theoretical /Experimental)	K_{IC} (mPa.$\sqrt{m}$)
Dolanit 11	0	650	23.36	23	23	0.985	0.287
	1	690	302.27	307.12	829.22	1.016	0.309
	3	1628	914.5	1021	3082.5	1.116	0.729
	5	2813	2465.5	2407.8	7023.8	0.98	1.259
	6	3454	3116	2853.3	8624.4	0.92	1.546
Dolanit 10	0	650	23.36	23	23	0.985	0.287
	1	1184	197.58	193.9	511.2	0.98	0.53
	2	2072	329.34	371.1	854.8	1.126	0.928
	3	2615	530.59	560.4	1819.6	1.056	1.171
E-glass	0	650	23.36	23	23	0.985	0.287
	1	1826	419.1	447.8	2080.6	1.07	0.818
	2	2763	546.15	614	2118.8	1.12	1.237
	3	3010	584.2	596.3	2139.5	1.02	1.348

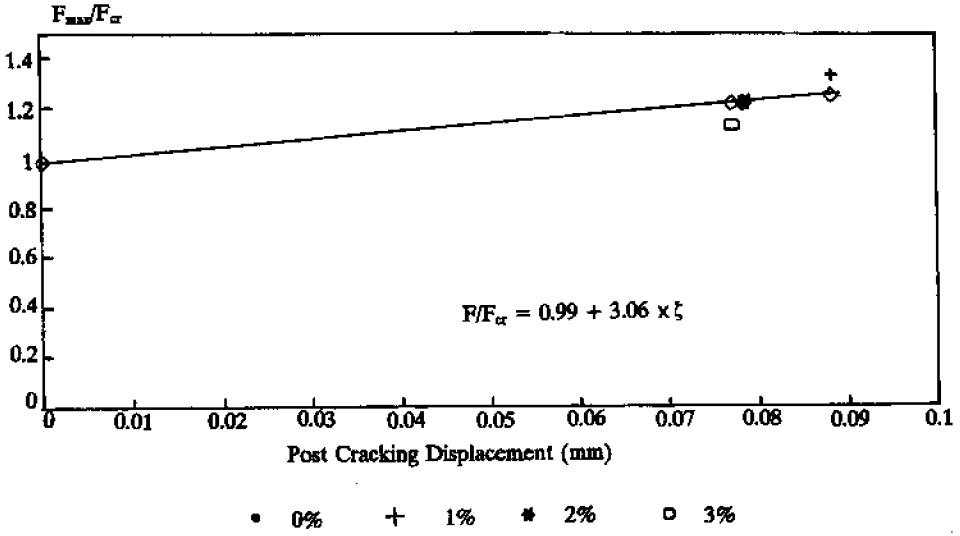

Fig.5. Variation of post-cracking displacement with post-cracking load up to maximum load for notched Dolanit 10 fibre reinforced beam.

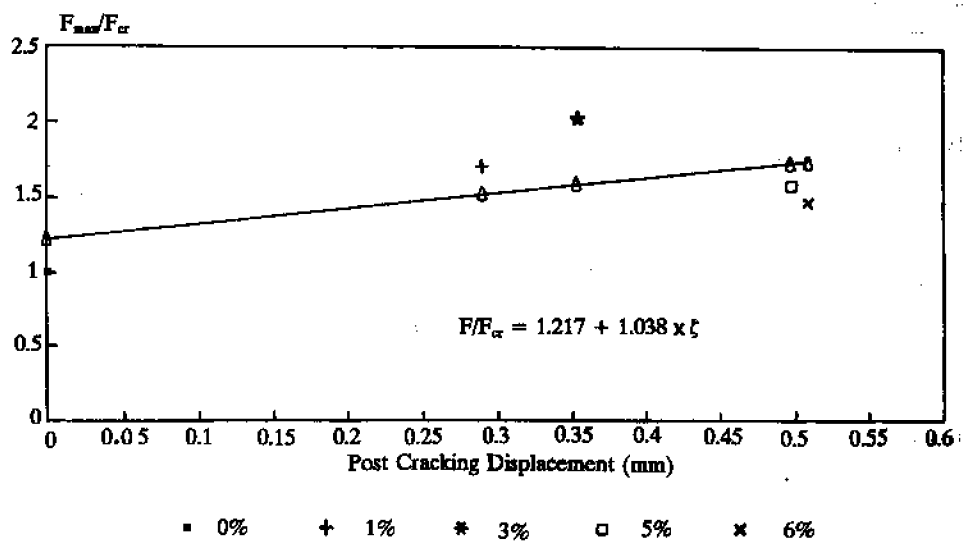

Fig.6. Variation of post-cracking displacement with post-cracking load up to maximum load for notched Dolanit 11 fibre reinforced beam.

between the theoretical and experimentally observed energy absorption capacities is good

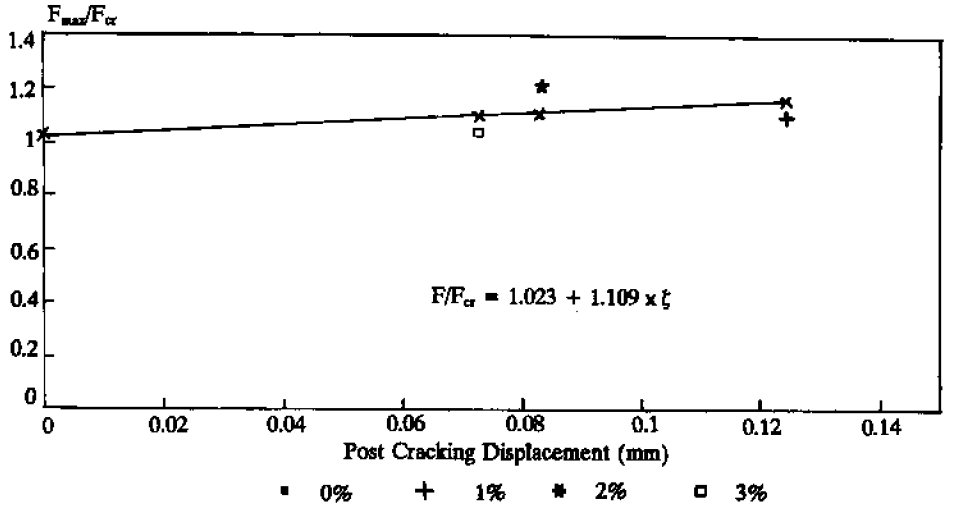

Fig.7. Variation of post-cracking displacement with post-cracking load up to maximum load for notched E-glass fibre reinforced beam.

considering the inherent scatter of results associated with cement-based composites. It appears that with glass fibre composites, the principle of energy absorption is mainly based on an increase in F_{cr} rather than the deformability of the material after the maximum load is reached.

The amount of energy absorption of composites is related to the type of failure. When fibres are pulled out from the matrix, the composite absorbs much more energy than when fracture of fibres occurs. In other words, around the critical length (lc) of fibres, the energy absorption will be maximum.

The total energy absorption capacity of these types of fibre reinforced cementitious composites is shown in Figure 8 as a function of fibre volume. From Figure 8, it was concluded that the total energy absorption capacity of these composites was increased with increasing volume fraction of fibres.

Stress intensity factors (K_I) were calculated from the force deflection curves using the Strawley equation [9] as below. For three point bend specimens:

$$K_I\, tw^{1/2}/P = 3(S/w)\,\alpha^{1/2}\{1.99-\alpha(1-\alpha)(2.15-3.93\alpha+2.7\alpha^2)\}/\,2(1+2\alpha)(1-\alpha)^{3/2} \quad (8)$$

Where α =a/w, t is the specimen thickness, w is the specimen width, α is the crack length, S is the support span and P is the applied load. In this work, the critical stress intensity factor/(K_{IC}) up to just initiation of cracking ($P=F_{cr}$) was calculated. The results are presented in Table 3 and depicted in Figure 9. Figure 9 Shows that the fracture stress of the fibre reinforced cementitious composites increases with volume fraction of fibres.

CONCLUSIONS

Polymeric fibres used in this work to reinforce cement can arrest any advancing cracks by applying pinching forces at the crack tips, thus delaying their propagation across the matrix and creating a distinct slow crack propagation stage and thus increasing ductility or toughness of cementitious composites.

From the higher energy of fracture or, in fact, higher fracture toughness obtained with

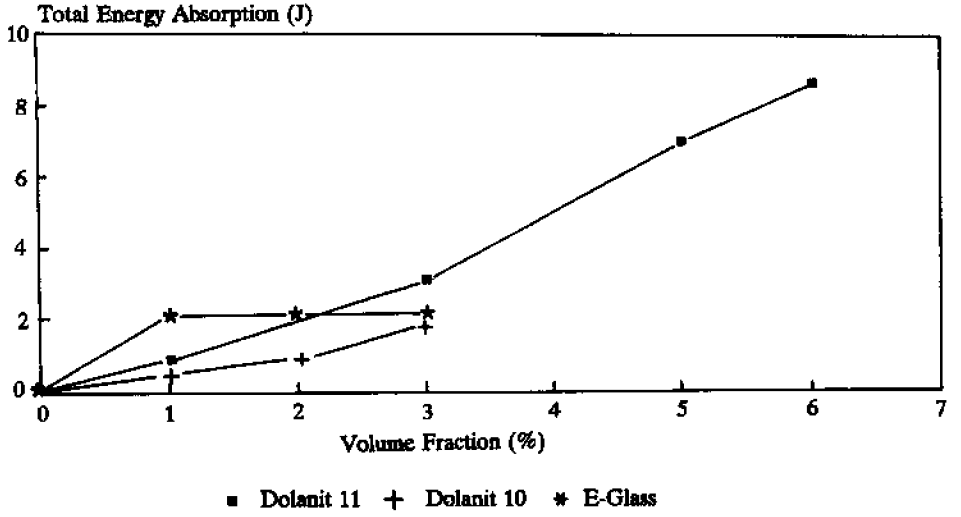

Fig.8. Variation of total energy absorption with volume fraction for fibre reinforced beams.

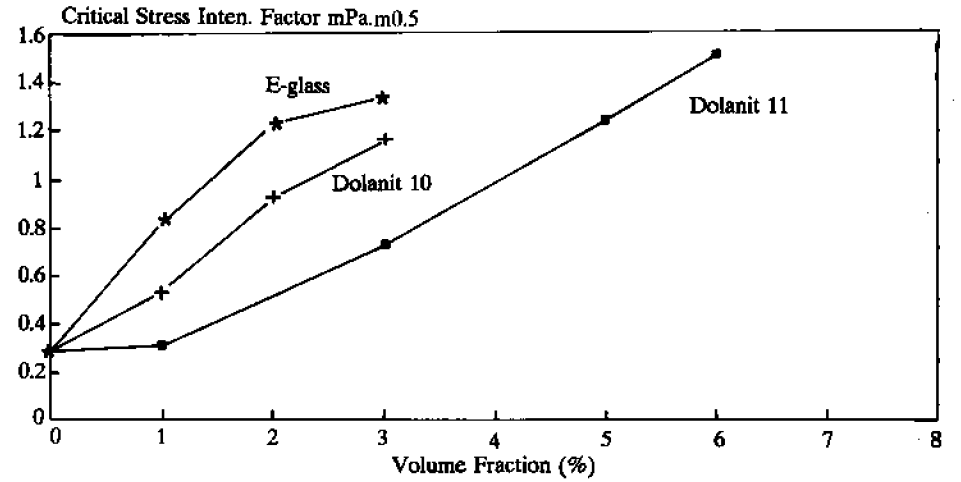

Fig.9. Variation of K_{IC} with volume fraction for notched Dolanit 10, Dolanit 11 and E-glass fibre reinforced beams.

respect to other fibres for Dolanit 11-incorporated cement it can be concluded that a pull-out mechanism occurs in fracture for this type of fibre reinforced composite.

Moreover, the aforementioned method of analysis enables the evaluation of the energy absorption capacity in terms of the maximum load, the specimen compliance and the deflection at

maximum load. The validity of the analysis is justified by the close agreement between the theoretical experimental results. Equations (5), (6)and (7) show that the relationship between F/F_{cr} and ζ is independent of the fibre volume which results in considerable simplicity of analysis.

SYMBOLS AND ABBREVIATIONS

C = Specimen compliance
F = Load
F_{cr} = Load at the initiation of crack length increase
F/F_{cr} = Load increase beyond stage one up to maximum load
ζ = Post cracking displacement
ζ_m = Maximum load displacement less than that corresponding to F_{cr}
E_1 = Energy absorbed during the first stage
E_2 = Energy absorption during the sub-critical crack growth
E_T = Total energy absorption during the first and second stage
K_{IC} = Critical stress intensity factor
t = Specimen thickness
w = Specimen width
a = Crack length
S = Support span
P = Load
α = a/w

ACKNOWLEDGEMENTS

The tests reported in this work form part of a wider study concerning the mechanics and behaviour of fibre-cement composites as an M.Sc. project. The project was supported by the Polymer Research Center and the Building and Housing Research Center of Iran. The authors would like to express their appreciation to the above mentioned organisations for their financial support.

REFERENCES

1 Hsu, T.T.C., et al. *Microcracking of Plain Concrete and the Shape of the Stress-Strain Curve. J. Amer. Concr. Inst.*, **60**, 209 (1963).

2 Swamy, R.N., et al. *Influence of the Methods of Fabrication on Strength Properties of Steel Fibre Concrete.* RILEM Materials and Structures, **52**, 243 (1976).

3 Glucklich, J., et al. *Size as a Factor in the Brittle-Ductile Transition and the Strength of Some Materials.* International Journal of Fracture Mechanics, **3**, 278 (1967).

4 Swamy, R.N., et al. *Fracture Mechanism in Concrete Systems Under Uniaxial Loading.* Cem. and Concr. Res. **3**, 413 (1973).

5 Swamy, R.N., et al. *A Theory for the Flexural Strength of Steel Fibre Reinforced Concrete.* Cem and Concr. Res., **4**, 313 (1974).

6 Davis, J.S. "*Fibre Reinforced Materials: Design and Engineering Applications*", Institution of Civil Engineers, London (1977).

7 Naaman, A.E., et al. *A fracture Model for Fibre Reinforced Cementitious Materials.* Cem. and concr. Res. **3**, 397(1973).

8 Neville, A.M., et al. "*Concrete Technology*", Longman Scientific & Technical Press, UK (1990).

9 Paipetis, S.A., et al., "*Engineering Applications of New Composites*", Omega Scientific, UK (1988).